Journal of Structural Geology, Vol. 9, No. 5/6, pp. 635 to 646, 1987
Printed in Great Britain

0191-8141/87 $03.00 + 0.00

Bulk kinematics from shear zone patterns: some field examples

DENIS GAPAIS, PASCAL BALE, PIERRE CHOUKROUNE, PETER R. COBBOLD, YAMINA MAHJOUB * and DIDIER MARQUER

Laboratoire de Géologie Structurale, Centre Armoricain d'Etude Structurale des Socles (CNRS), Université de Rennes, 35042 Rennes Cedex, France and * Département de Géologie, U.S.T.H.B., Alger, Algéria

(*Received* 23 *June* 1986; *accepted in revised form* 10 *February* 1987)

Abstract—Geological deformations which are statistically homogeneous at bulk scale (e.g. the macroscale) are often localized into arrays of narrow shear zones at a smaller scale (e.g. the mesoscale). This paper shows that shear zone patterns can be used to estimate both a bulk finite strain ellipsoid and aspects of the bulk deformation history. We describe examples of heterogeneously deformed granitic rocks which reveal the following features. (1) Shear zones show preferred orientations. (2) There are correlations between shear zone orientations and directions and senses on shear. (3) For areas that have undergone coaxial deformation histories, shear zone patterns have orthorhombic symmetries directly related to strain ellipsoid shape. (4) For areas that have undergone non-coaxial deformation histories, shear zone patterns have a lower symmetry. (5) For areas that have undergone bulk simple shear, shear senses on shear zones are consistent with the bulk shear sense. Results are compared with predictions of kinematic models involving slip along inextensible fibres and sheets. According to these models, preferred orientations of slip surfaces track surfaces of no finite extension of the bulk strain ellipsoid, whereas slip directions track directions of large shear in the bulk strain ellipsoid. There are good correlations between preferred orientations of shear zones and fibre models.

INTRODUCTION

IN MANY deformed rocks, especially those with an initially homogeneous and isotropic structure (e.g. plutonic rocks), deformation is highly localized into band-like shear zones. These zones generally form anastomosing arrays, enclosing domains with smaller and more homogeneous strain. At the bulk scale, zones can be described as discontinuities in the displacement field, in other words, as slip surfaces; but, at a smaller scale, they are in fact coherent transition zones with continuous deformation gradients. Once developed, active shear zones must combine together, so as to accommodate most of the total deformation, irrespective of the deformation mechanisms that operate at the grain scale. Accordingly, one expects strong relationships between the geometry of a given shear zone pattern and the corresponding average (mean) deformation at bulk scale. By geometry we mean, in particular; (i) preferred orientations of shear zones; and (ii) changes in direction, sense and amount of shear according to shear zone orientation.

Relationships between shear zone patterns and bulk strain have been examined by Mitra (1979) in a strain analysis of basement granitic rocks. His approach compares with those developed for intracrystalline slip systems (Taylor 1938, Lister *et al.* 1978) or brittle faults (Oertel 1965, Freund 1974, Reches 1983). He deduced that five independent sets of shear zone orientations are required to accommodate a general bulk homogeneous strain. Thus, Mitra extended the von Mises criterion from lattice scale to rock scale and from discrete slip planes to ductile shear zones. Several kinematic models for accommodating a bulk plane strain have been derived from natural shear zone patterns (Ramsay 1980, Bell 1981). However, all these studies are mainly supported by two-dimensional observations. They do not provide critical data to define: (i) relationships between shear zone preferred orientations and the bulk strain ellipsoid; and (ii) kinematic factors which can control the evolution of shear zone patterns during progressive deformation.

Concerning the relationships between shear zone patterns and deformation history, few data are available and these remain essentially two-dimensional (see Collins & De Paor 1986). A coaxial history is expected to result in symmetric conjugate shear zones. In contrast, experiments (Hoeppener *et al.* 1969, Tchalenko 1970, Mandl *et al.* 1977, Logan *et al.* 1981), numerical models (Priour 1985) and field examples (Berthé *et al.* 1979, Platt & Vissers 1980) all show that progressive simple shear results in the predominance of one set of shear zones over the conjugate set (e.g. *C* surfaces, Berthé *et al.* 1979). Faulting experiments further emphasize that an imposed bulk simple shear can result in patterns of anastomosing zones which are locally complex, with several sets (e.g. Riedel experiments, see Tchalenko 1970). Comparable patterns are found in natural sheared rocks (Bell 1981, Simpson 1983, Gapais & Jegouzo 1985) and both their mechanical and kinematic significances are still unclear.

The aim of the present paper is to describe how shear zone patterns can be used as qualitative shear criteria and strain markers at the bulk scale. We concentrate on their use as kinematic indicators, rather than discuss possible variations in geometry depending upon mechanical effects. The latter question will be left for further publications.

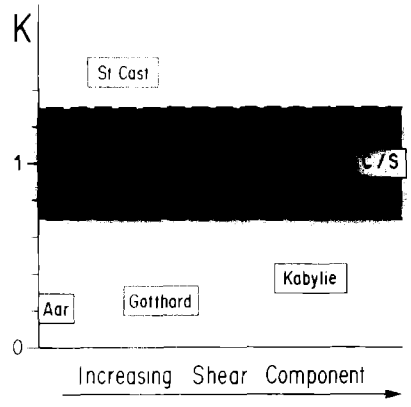

Fig. 1. The five examples of studied shear zone patterns in a schematic kinematic reference frame relating shape parameter (K) of the bulk strain ellipsoid [$K = (\lambda_1/\lambda_2 - 1)/(\lambda_2/\lambda_3 - 1)$, Flinn 1962; $\lambda_1 \geq \lambda_2 \geq \lambda_3$, principal stretches, Truesdell & Toupin 1960] to qualitative degree of non-coaxiality of bulk deformation history (qualitative estimates from local tectonics and results presented in this paper).

We present five examples of granitic rocks from various crustal structures and deformed under various kinematic conditions (Fig. 1). Each example has undergone one major progressive deformation. The deformed material within shear zones can be compared with its undeformed or weakly deformed equivalent outside the zones. We summarize published data from: (i) areas in the Aar Massif (Central Alps) which are deformed in the flattening field (Choukroune & Gapais 1983); and (ii) typical C–S granites with deformation histories close to simple shearing, special reference being made to granites from South Armorican Shear Zone (Berthé *et al.* 1979). We describe new structural observations from: (i) areas in the Gotthard Massif (Central Alps); (ii) granitic rocks from eastern Kabylie (N.E. Algeria); and (iii) granitic rocks from the St Cast area (northern Brittany). Observed shear zone patterns are compared with basic predictions of kinematic models briefly summarized in the next section.

KINEMATIC MODELS

The kinematic models we refer to in this paper are fibre models where deformation occurs by slip along discrete inextensible slip systems. For such extreme mechanical conditions, preferred orientations are largely governed by kinematic factors. Fibre models and their applications to various kinds of natural slip systems (e.g. bedding planes, lattice planes or faults) are described in detail elsewhere (Cobbold & Gapais 1987, Gapais & Cobbold 1987) and will not be developed here. They predict the following basic relationships between preferred orientations of active slip systems and bulk kinematics.

(1) At a local scale, slip lines tend to occupy orientations along which the stretching is minimized and the shearing is maximized. With respect to the bulk strain ellipsoid, preferred orientations of inextensible fibres track orientations of no finite extension but are biased towards directions of large shear.

(2) Corresponding preferred orientations of slip surfaces are approximately tangential to the surface of no finite extension.

(3) A large strain with a large component of simple shear requires a maximum concentration of slip lines close to the bulk shear direction. For simple shearing, the average (mean) fibre direction must be parallel to the bulk shearing direction.

ANALYTICAL PROCEDURE

The shear zones or shear bands that we have considered have the following characteristics (Fig. 2).

(1) They are millimetric to decimetric in width.

(2) They are all ductile zones contemporaneous with major deformation and metamorphism in the considered areas. Occasional brittle faults, not clearly related either geometrically or chronologically to the regional deformation, have not been considered.

(3) They are local perturbations of a more homogeneous and penetrative strain field expressed by a regional foliation and a regional stretching lineation (see Fig. 2). These are defined by preferred alignments of constitutive minerals or grain aggregates (feldspar porphyroclasts, micas, quartz ribbons) and by preferred orientations of deformed xenoliths. Foliation and lineation have been considered as defining the principal strain axes ($\lambda_1, \lambda_2, \lambda_3$) and are used as a local reference frame.

(4) Within high strain shear zones, stretching lineations can parallel striations which underline the local slip direction.

Where present, deformed xenoliths have been used to estimate penetrative strains at outcrop scale. Measured xenoliths are fine-grained magmatic inclusions of basic composition. They are centimetric to decimetric in size. Mean axial ratios of a given population measured within principal strain planes were generally obtained from plots of lengths of long axis versus short axis, using the least squares method (Ramsay 1967, p. 193). In most cases, this method proved sufficiently accurate because: (i) plots showed a good alignment of points along a straight line passing through the origin; and (ii) orientations of xenoliths within a given section were approximately constant and parallel to the lineation and (or) the trace of the foliation. However, the R_f/ϕ method (Dunnet 1969) has been used where xenoliths showed significant misorientations (low strain areas). The lack of schistosity refraction across all measured xenoliths attested to low viscosity contrasts between markers and matrix, which yields relatively good estimates of strain. Measurements were made on several outcrops within the St Cast, Aar and Gotthard granites. They contribute to assess the range of finite strain ellipsoid shapes across the studied shear zone patterns.

The local geometry of a given shear zone is described by the shear direction L, the normal N to the shearing plane (shear zone walls), and the normal M to the plane of shear (Fig. 3) (definitions following Truesdell & Toupin 1960). M is a useful characteristic direction as its

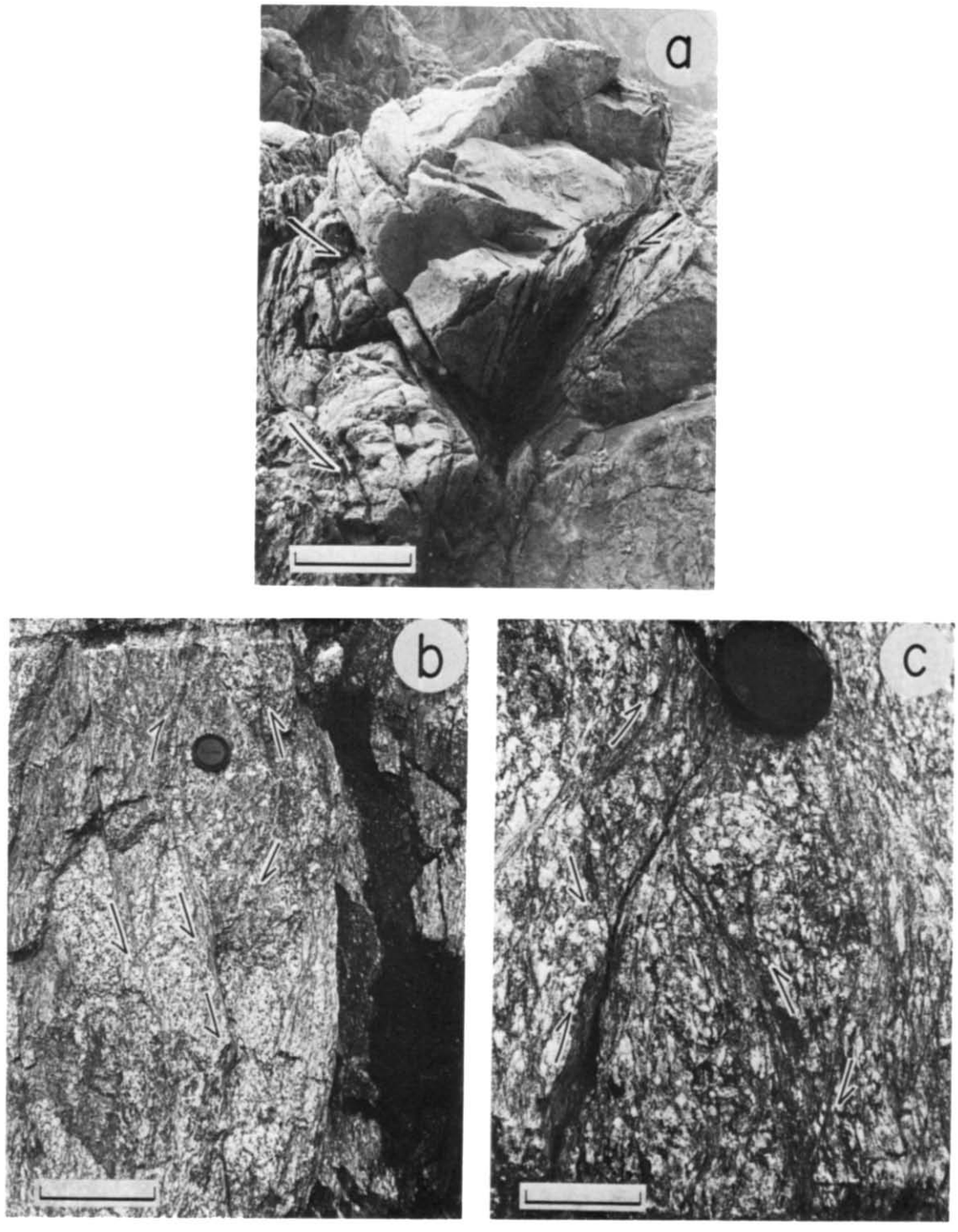

Fig. 2. Examples of various scale shear-zone patterns in the granites studied. (a) St Cast granite showing an undeformed domain (middle) surrounded by conjugate shear zones (arrowed); scale bar is 75 cm. (b) and (c) Aar granite showing patterns of conjugate shear zones (arrowed) similar in both $\lambda_1\lambda_3$ plane (b) (scale bar is 20 cm) and $\lambda_2\lambda_3$ plane (c) (scale bar is 5 cm).

(*continued overleaf*)

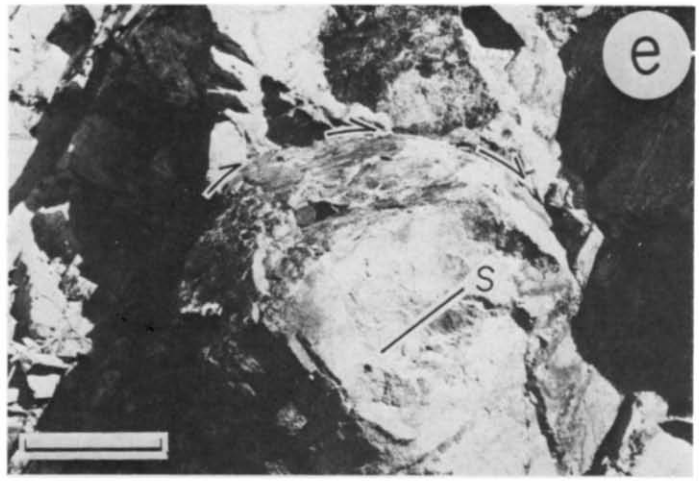

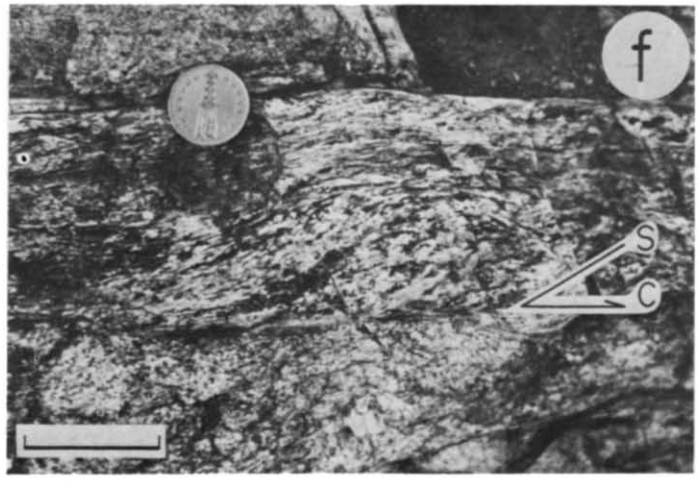

Fig. 2 (*continued*) (d) Gotthard granite showing a lens-shaped domain of weakly deformed material (bright area, middle) surrounded by orthogneiss with subvertical foliation (dark areas); $\lambda_1\lambda_3$ plane; scale bar is 4 m. (e) and (f) Kabylie granites (south to the right). (e) lens of weakly foliated granite (schistosity *S*) surrounded by a curved shear zone with constant sense of shear (arrowed); $\lambda_1\lambda_3$ plane; scale bar is 20 cm. (f) Typical *C*–*S* structures (shearing plane *C* and schistosity *S*) and shear strain gradient from weakly deformed granite (bottom) to ultramylonite within S-vergent mylonitic thrust zone; $\lambda_1\lambda_3$ plane; scale bar is 6 cm.

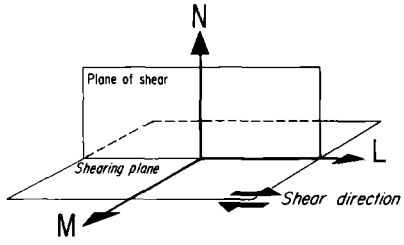

Fig. 3. Conventions used to describe local shear zone attitude by three perpendicular directions; L shear direction; M, pole to plane of shear; N, pole to shearing plane (Truesdell & Toupin 1960).

attitude depends on those of both slip line and slip plane. Its use to describe populations of slip surfaces was introduced by Arthaud (1969) for brittle faults. In the following sections, orientation patterns of L, M and N will be shown on stereograms projected into the $\lambda_1\lambda_3$ bulk strain plane. Each data set will be compared with orientation patterns predicted by fibre models for a coaxial deformation and a suitable bulk strain ellipsoid for the considered area. For a given strain ellipsoid, the surface of no finite extension, and orientation domains where material lines have suffered a large amount of parallel shear, outline favourable orientations of inextensible slip lines (see also Gapais & Cobbold 1987). Accordingly, the surface normal to the surface of no finite extension and orientation domains of poles to planes affected by a large amount of parallel shear outline favourable orientations of poles to inextensible slip planes.

ST CAST GRANITES

This first example concerns basement granitic rocks outcropping in St Cast, northern Brittany, France (area of the 'pointe de St Cast'; co-ordinates 262.5–114.7, French topographic map I.G.N. No. 1015). These rocks are considered late Proterozoic in age (Jeannette 1972) and were deformed at about 580 Ma during the Cadomian orogeny.

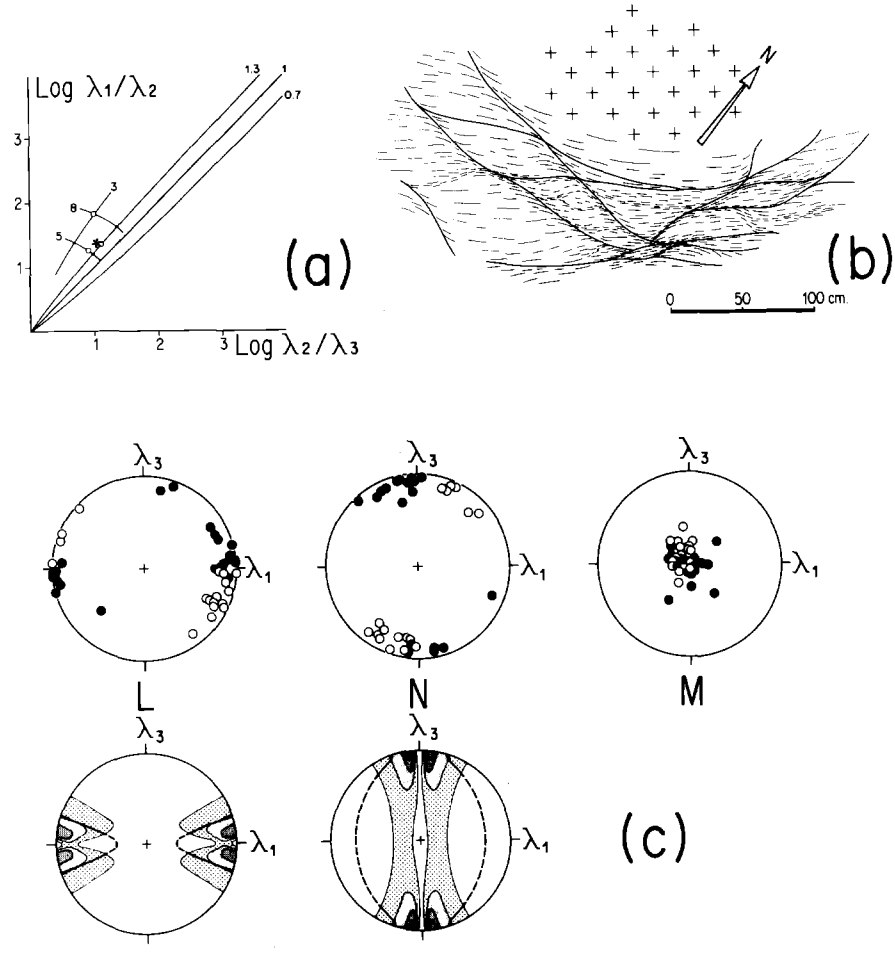

Fig. 4. St Cast granites. (a) Logarithmic plot (base e) of strain measurements from deformed xenoliths; curves are for particular constant values of non-logarithmic K (0.7, 1.3 and 3) or r (5 and 8) parameters; shaded area ($0.7 \leqslant K \leqslant 1.3$) represents domain of plane-strain type ellipsoids. (b) Map showing relationships between regional foliation (thin lines), conjugate shear zones (thick lines) and undeformed domain (crosses) in the $\lambda_1\lambda_3$ plane. (c) Equal-area stereographic projections showing distributions of L, N and M directions, together with predictive diagrams for coaxial deformation and representative strain ellipsoid [$K = 1.5$, $r = 6$; star on (a)]; solid and open circles are sinistral and dextral zones, respectively; L predictive diagram shows surface of no finite extension (heavy lines) and contours of shear strain along lines; N predictive diagram shows orientations of poles to planes tangent to surface of no finite extension (heavy lines) and contours of shear strain along planes; contours are for percentages of maximum amount of shear (30, 50, 70 and 90%) for the considered ellipsoid.

Penetrative strains estimated from deformed xenoliths in the area are slightly constrictive, but close to the plane-strain field ($1.3 \leqslant K \leqslant 3$; K, shape parameter of strain ellipsoid, Flinn 1962) (Fig. 4a). Measured strain intensity parameters r range between 5 and 8 ($r = \lambda_1/\lambda_2 + \lambda_2/\lambda_3 - 1$, Watterson 1968; $\lambda_1 \geqslant \lambda_2 \geqslant \lambda_3$, principal stretches). The shear zone pattern described here corresponds to an outcrop area of about 200 m^2 where measured K values are around 1.5 (star on Fig. 4a). The regional schistosity strikes NE–SW and is subvertical. The stretching lineation is subhorizontal.

Shear zones anastomose around domains of locally undeformed and isotropic material (Figs. 2a and 4b). In the $\lambda_1\lambda_3$ plane, they are often rather straight except where they intersect each other. The overall pattern is that of lozenge-shape domains bounded by two sets of conjugate shear zones with opposite sense of shear and intersectioning about λ_2. This pattern is revealed by stereograms of L, N and M orientations (Fig. 4c). Poles N to conjugate shears are concentrated within the $\lambda_1\lambda_3$ plane and tend to cluster around two maxima at low angle to λ_3. Shear directions L also lie within the $\lambda_1\lambda_3$ plane. Accordingly, poles M to planes of shear are concentrated about λ_2.

The pattern is in fact consistent with that expected for plane strain: shear surfaces tend to be conjugate planes at low angle to the schistosity; shear directions are consistently oriented within the $\lambda_1\lambda_3$ plane, so that they accommodate bulk stretch along λ_1 but not along λ_2.

For constrictive strain ellipsoids, orientations of N such that a significant amount of shear is accumulated along slip planes correspond to an open elliptical cone centered about λ_1 (see Gapais & Cobbold 1987). Such a pattern appears on the predictive diagram of Fig. 4(c) which is drawn for a slightly constrictive ellipsoid ($K = 1.5$), but is not observed on the measured pole figure: poles N tend to concentrate close to orientations for which: (i) the amount of shear along planes exceeds 50% of the maximum amount of shear for the considered strain ellipsoid; and (ii) shear zones have suffered a large amount of parallel shear together with a minimum parallel stretch (overlap domain between orientations of large amount of shear and surface of no finite extension on pole figure). Nevertheless, field evidence shows that shear zones anastomose in the $\lambda_2\lambda_3$ plane (e.g. Fig. 2a). This results locally in rod-shaped low-strain domains between shear zones, especially in areas of large bulk strain. Such local patterns imply a scattering of poles N to shearing planes about λ_1, which is consistent with a constrictive strain.

AAR GRANITES

The Aar Massif, situated in Central Switzerland, belongs to the External Crystalline Massifs of Central Alps. It comprises granitic rocks of late Hercynian age deformed under greenschist metamorphic conditions during the Alpine orogeny (Steck 1968, 1984, Choukroune & Gapais 1983). The outcrops described here consist of granite and granodiorite (Grimsel granodiorite) of the central part of the Aar Massif (Aar Valley, north of Grimsel Pass; co-ordinates 664.7–159.9, Swiss topographic map No. 1230).

Strain measurements from deformed xenoliths in the area (see also Choukroune & Gapais 1983) yield ellipsoids of the flattening type ($0.03 \leqslant K \leqslant 0.7$) irrespective of strain intensity (Fig. 5a). The latter varies from low values outside shear zones ($r \geqslant 1.3$) to extremely high values within ultramylonites (measured r parameters up to 22) (Fig. 5a). The regional schistosity has a remarkably constant strike around N70°. Both schistosity and stretching lineation are generally subvertical.

Low-strain domains between strongly deformed zones define lenses flattened parallel to the regional schistosity ($\lambda_1\lambda_2$ plane) (Figs. 2b & c and 5b & c). Lenses are slightly elongate parallel to λ_1, but the overall pattern is rather close to axisymmetric about λ_3. Consistently, poles N to shear surfaces tend to define a small-circle pattern centred about λ_3 (Fig. 5d). This high degree of symmetry is expressed by curved shear surfaces with a comparable geometry in both $\lambda_1\lambda_3$ and $\lambda_2\lambda_3$ principal planes (Figs. 2b and c and 5b & c).

The distribution of shear directions L is also rather symmetric (Fig. 5d). Shear directions tend to track a small circle at low angle to the $\lambda_1\lambda_2$ plane and centered about λ_3. This pattern outlines the overall 3-D shape of lenses and further shows that shear directions tend to be radially disposed on lens surfaces (see Fig. 10). The sense of shear varies consistently on curved shear surfaces, according to their local orientation with respect to bulk principal strains: conjugate shear surfaces at high angle to the $\lambda_1\lambda_3$ plane and intersecting about λ_2 show conjugate shear senses about λ_1 (open and closed circles, Fig. 5d); conjugate shear surfaces at high angle to the $\lambda_2\lambda_3$ plane and intersecting about λ_1 show conjugate shear senses about λ_2 (open and closed squares, Fig. 5d). Changes in shear direction according to shear surface orientation yield a characteristic scattering of poles M to planes of shear in all orientations close to the mean regional schistosity $\lambda_1\lambda_2$ (Fig. 5d).

A good consistency is observed between measurements and predictions of fibre models (Fig. 5d) for K and r values representative of the study area (star on Fig. 5a). Models show that all orientations close to surfaces of no finite extension are also orientations along which a large amount of shear is accumulated (50% of the maximum amount of shear, Fig. 5d). This accounts for the observed scatter of shear directions at high angles to λ_3. Similar correlations can be made for poles to shear surfaces.

The lens-type shear zone pattern clearly accounts for finite flattening strains, as recorded by classical strain markers (Fig. 5a). In a previous paper, two of us (Choukroune & Gapais 1983) have shown that this pattern was observed at all scales and for various amounts of bulk strain together with a constant orientation of the regional schistosity (Fig. 5c). They interpreted this as a tendency for the shear zone pattern to remain axisymmetric about a constant shortening direction during progressive defor-

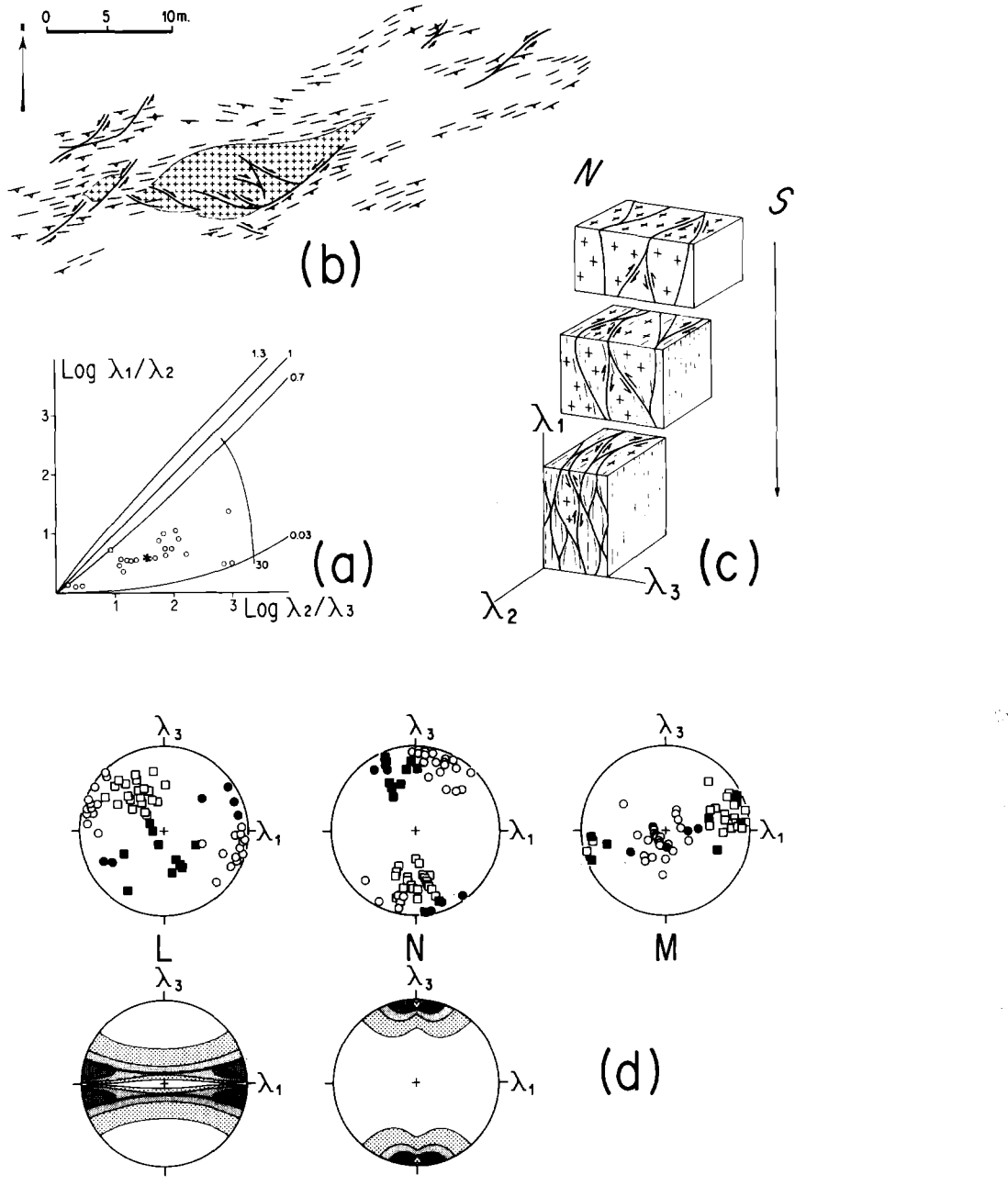

Fig. 5. Aar granites (data from Choukroune & Gapais 1983). (a) Logarithmic plot of strain measurement from deformed xenoliths. (b) Foliation map showing lens-shaped undeformed domain (crosses) surrounded by curved shear surface in the $\lambda_2\lambda_3$ plane. (c) Schematic block diagrams showing 3-D shear zone pattern for three stages of increasing bulk strain; conjugate zones occur in both $\lambda_1\lambda_3$ and $\lambda_2\lambda_3$ planes. (d) Equal-area stereographic projections for L, N and M directions together with predictive diagrams for coaxial deformation and representative strain ellipsoid [$K = 0.21$, $r = 5.45$, star on (a)]; open and solid circles are for conjugate zones intersecting at high angle to λ_1; open and solid squares are for conjugate zones intersecting at high angle to λ_2. See caption of Fig. 4 for further details.

mation. Consequently, they proposed a model of orthogneiss development by bulk coaxial progressive flattening (Fig. 5c). The good consistency observed between the shear zone pattern and fibre models for coaxial flattening supports this interpretation.

GOTTHARD GRANITES

Like the Aar granites, the Gotthard granites belong to the External Crystalline Massifs of the Central Alps. Their deformation is also of Alpine age and occurred under metamorphic conditions of the amphibolite facies (Frey *et al.* 1980). Results described below relate to granite outcrops (Fibbia granite and Gamsboden granite) located north of the Gotthard Pass (co-ordinates 686–157.7, Swiss topographic map No. 1251).

The regional foliation has a constant average N60° strike. It is subvertical or dips steeply southward. The associated stretching lineation plunges steeply. Finite strains measured from deformed xenoliths are of flattening type ($0.02 \leqslant K \leqslant 0.5$) (Fig. 6a) as in the Aar granite (Marquer & Gapais 1985, Marquer 1987).

The overall shear zone pattern is also comparable

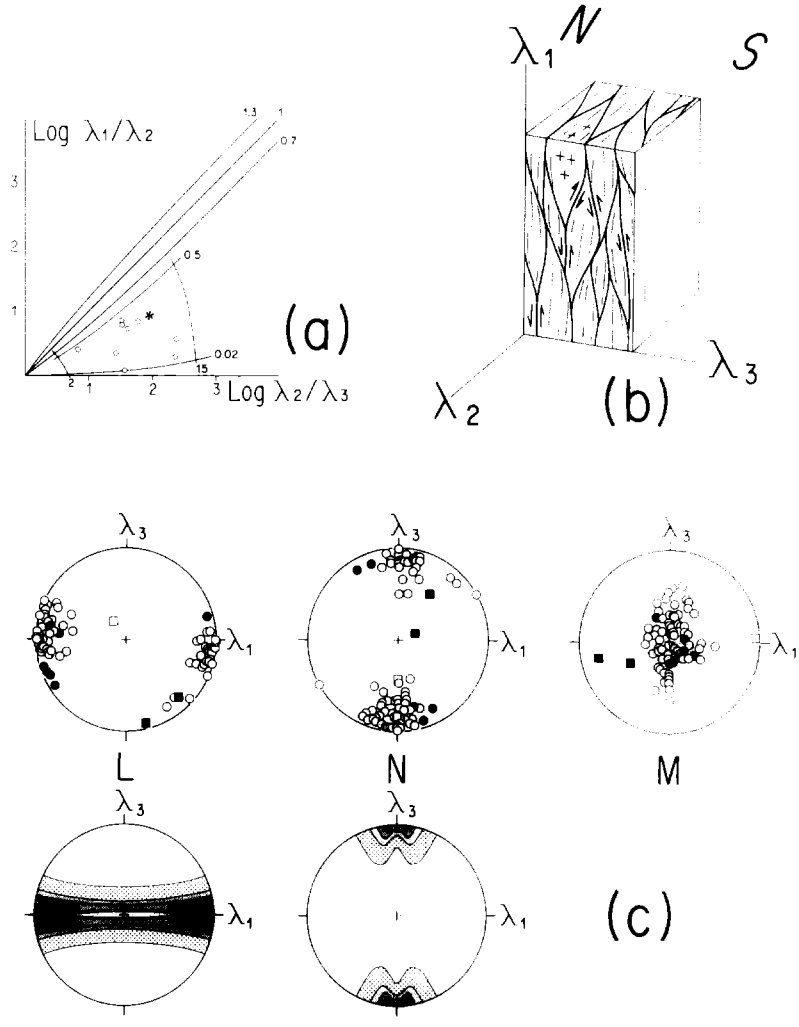

Fig. 6. Gotthard granites. (a) Logarithmic plot of strain measurements from deformed xenoliths. (b) Schematic block-diagram showing 3-D shear zone pattern; most shear zones have a northward sense of shear [open circles on (c)]. (c) Same caption as Fig. 5(d); predictive diagrams are for coaxial deformation, $K = 0.25$ and $r = 9$ [star on (a)].

to that of the Aar granites. It consists of mylonite zones surrounding lenses of lower strain (Figs. 2d and 6b). However, the following major differences are observed.

(1) Lenses are strongly flattened within the regional schistosity (Fig. 6b). This is expressed by a strong clustering of poles N to shear surfaces towards λ_3 (Fig. 6c). Fibre models predict such a clustering for a high flattening strain (Fig. 6c, $r = 9$; star on Fig. 6a) compared with that quoted for the Aar example (Fig. 5d, $r = 5.45$; star on Fig. 5a). Hence, undeformed or weakly foliated domains are uncommon in the study area of the Gotthard massif, whereas they are well developed in the Aar granite.

(2) Lenses are asymmetric, resulting in the following major differences between observed patterns and predictions of fibre models for coaxial flattening (Figs. 6b & c and 10). (a) The schistosity itself has locally acted as a shearing plane (Fig. 6b). This results in the occurrence of poles N to shear surfaces parallel to λ_3 and of shear directions L parallel to λ_1 (Fig. 6c). This, combined with a high bulk strain intensity, accounts for the poor correlation found between observed and expected distributions of N. (b) Shear directions are shifted towards the principal stretch direction (Fig. 6c). Conjugate shears about λ_2 (squares on Fig. 6c) are uncommon compared with the Aar example (see Fig. 5d), although K values are comparable in both cases. Consequently, poles M to planes of shear scattered along the $\lambda_1\lambda_2$ plane are uncommon (compare Figs. 6c and 5d). The scattering along $\lambda_1\lambda_2$ is here replaced by an elongate concentration perpendicular to the maximum concentration of shear directions L (Fig. 6c). This characteristic change in the distribution of poles M reflects the development of a preferred orientation of shear directions L disposed on a lens-shaped shear surface (Fig. 10). (c) There is one dominant sense of shear along lens surfaces. The dominant set, including schistosity planes, corresponds to a northward sense of shear (Fig. 6b; open circles, Fig. 6c). The conjugate set is present (closed circles, Fig. 6c) but is poorly developed.

Lens asymmetry is interpreted as the result of a non-coaxial flattening (Fig. 10). It is consistent with a component of regional thrusting towards the north, as inferred from regional structural analysis (Marquer & Gapais 1985).

KABYLIE GRANITES

Granitic rocks here designated as Kabylie granites are observed within Hercynian basement rocks outcropping in eastern Kabylie, N.E. Algeria. They intrude a series of metamorphic orthogneisses and paragneisses. Emplacement and deformation ages are still unclear (Mahjoub & Gapais 1985). The particular area described here is situated south of Collo (co-ordinates 848–409.7, Algerian topographic map No. 13).

Good strain markers such as basic xenoliths are lacking in these granites; but mean aspect ratios of relict aggregates of quartz and feldspars within orthogneissic and mylonitic material are consistent with strains of the flattening type ($K > 0.3$, Fig. 7a).

The overall structure is sketched in Fig. 7(b) (similar patterns can be observed at various scales, which accounts for the lack of reference scale on this sketch). It corresponds to a major ductile S-vergent thrust zone of several tens of metres thick where local flat-lying thrust surfaces separate thicker domains with a locally steeply N-dipping foliation. The latter show domains of low strain surrounded by curved shear surfaces (Figs. 2e and 7b). South vergent *C–S* structures (Berthé *et al.* 1979) occur within flat-lying mylonitic shear zones (Figs. 2f and 7b).

The shear zone pattern is strongly asymmetric. All shear surfaces show a southward sense of shear irrespective of their attitude with respect to principal strains (Fig. 2e) (only closed circles on Fig. 7c). Nevertheless, poles N to shear surfaces tend to outline an incomplete small-circle pattern about λ_3. This reflects the occurrence of lens-shaped shear zone patterns (curved shear zones, Figs. 2e and 7b), as predicted by fibre models for flattening strains. Shear directions L tend to cluster in a single maximum oblique to the principal strain plane $\lambda_1\lambda_2$ (Figs. 7c and 10). The obliquity is consistent with an overall southward shear sense. According to orientations of L and N, poles M to planes of shear are concentrated about λ_2 (Fig. 7c). Nevertheless, the maximum concentration of M is slightly elongate perpendicular to the mean shear direction outlined by the preferred orientation of L directions. This is due to lens-shaped shear surfaces (compare with Figs. 6c and 10).

C–S GRANITES

C–S Structures within granitic rocks have been described by Berthé *et al.* (1979) as typical of progressive shearing deformation and are now recognized as most reliable shear criteria (see Simpson & Schmid 1983).

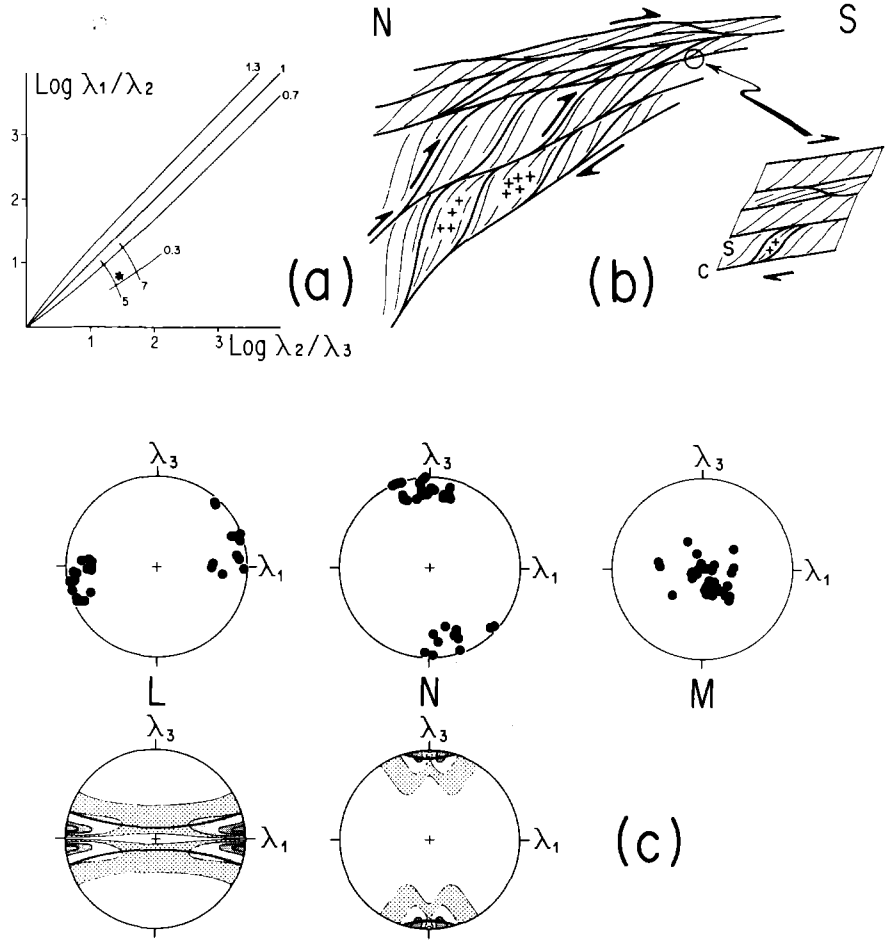

Fig. 7. Kabylie granites. (a) Logarithmic plot of strain estimate. (b) Sketch of overall shear zone pattern (heavy lines) and schistosity (thin lines) in the $\lambda_1\lambda_3$ plane. (c) Same caption as Fig. 5(d); closed circles are south-vergent shear zones; predictive diagrams are for coaxial deformation, $K = 0.35$ and $r = 5.7$.

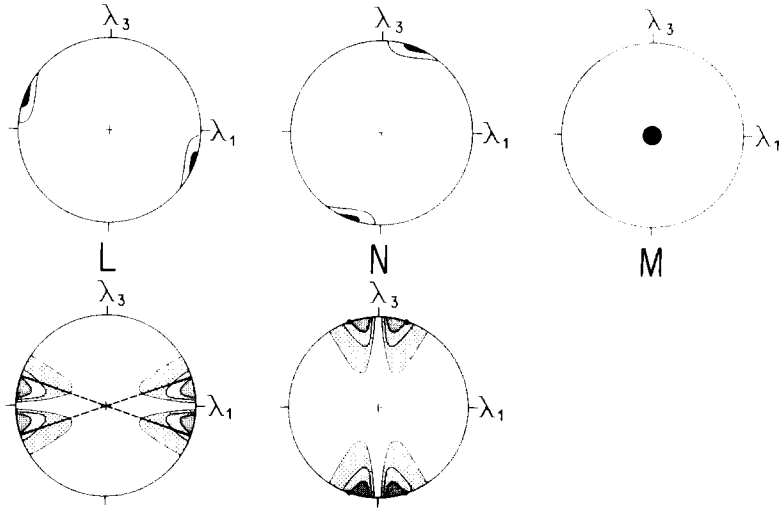

Fig. 8. Sketch of typical distributions of L, N and M directions within C–S granites. Predictive diagrams are for coaxial deformation, $K = 1$ and $r = 5$. See caption for Fig. 5(d).

Their geometry, as deduced from granites deformed by dextral transcurrent shearing along the South Armorican Shear Zone (Berthé *et al.* 1979), is sketched in Fig. 8.

One single set of shear surfaces is expressed. They are planar surfaces whose constant average orientation parallels the shear zone boundaries at a larger scale. They contain the bulk principal strain axis λ_2. Shear strain gradients are marked by a gradual rotation of the schistosity (S surfaces, $\lambda_1\lambda_2$ plane) towards the shearing planes (C surfaces) (Fig. 2f). The shear direction has a constant orientation in the $\lambda_1\lambda_3$ plane.

This geometry, with no variations along λ_2, is fully described in two dimensions ($\lambda_1\lambda_3$ plane). It thus suggests conditions of bulk plane strain. Hence the 3-D shapes of shadow zones around feldspar porphyroclasts within South Armorican granites also indicate plane strain (Berthé *et al.* 1979). In a study of sheared granites from Morocco, Lagarde & Choukroune (1982) provide quantitative strain data for a regional scale C–S shear zone. Their results indicate plane strain for a large range of strain intensities ($1.3 \leq r \leq 17$; Lagarde & Choukroune 1982). Predictive diagrams of Fig. 8 are drawn for a coaxial plane strain and a strain intensity parameter r of 5. Irrespective of the symmetry, they feature consistently the mean angular relationships between C and S as found in typical C–S orthogneisses (Berthé *et al.* 1979, Lagarde & Choukroune 1982) (a plane-strain ellipsoid with $r = 5$ yields $\gamma = 2.7$ in simple shear).

The occurrence of one single set of parallel shear planes which accommodate most of the total deformation is consistent with progressive simple shearing. Fibre models also show that the deformation must be simple shear if it is achieved by slip along only one set of parallel inextensible fibres (Cobbold & Gapais 1987, Gapais & Cobbold 1987). Simple kinematic comparison can be made with an isolated single crystal deforming by slip along a unique slip system. In the shear zone case, the active shear direction is imposed by boundary conditions, whereas it is imposed by crystallographic constraints in the crystal case; but in both cases, the active shearing plane tracks the unique fixed orientation of no stretching for a simple shearing deformation.

CONCLUDING REMARKS

Field data presented in this paper show that relevant kinematic inferences can be made from the 3-D analysis of ductile shear zone patterns. Our major conclusions are summarized in Figs. 9, 10 and 11.

Bulk finite strain vs shear zone pattern

Three-dimensional shear zone patterns vary consistently according to the shape of the bulk finite strain ellipsoid (Fig. 9). Furthermore, a mean strain ellipsoid can in principle be estimated at the scale of any domain size in which compatible shear zones define a consistent pattern. Flattened low-strain lenses surrounded by curved shear surfaces both in the $\lambda_1\lambda_3$ and $\lambda_2\lambda_3$ principal planes indicate the flattening field. Towards the plane-strain field, shear zones tend to become more planar and the patterns are different in the $\lambda_1\lambda_3$ and $\lambda_2\lambda_3$ principal planes. Lozenge-shaped arrays of anastomosing zones

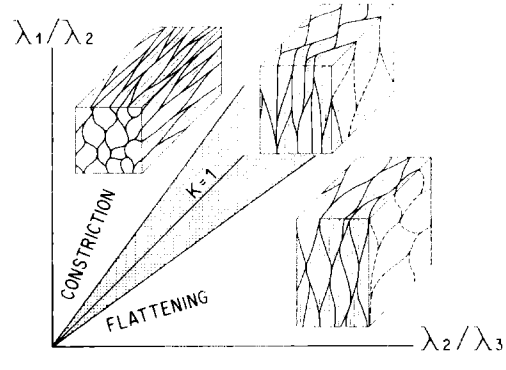

Fig. 9. Flinn diagram summarizing conclusions on relationships between shear zone pattern and bulk finite strain ellipsoid shape.

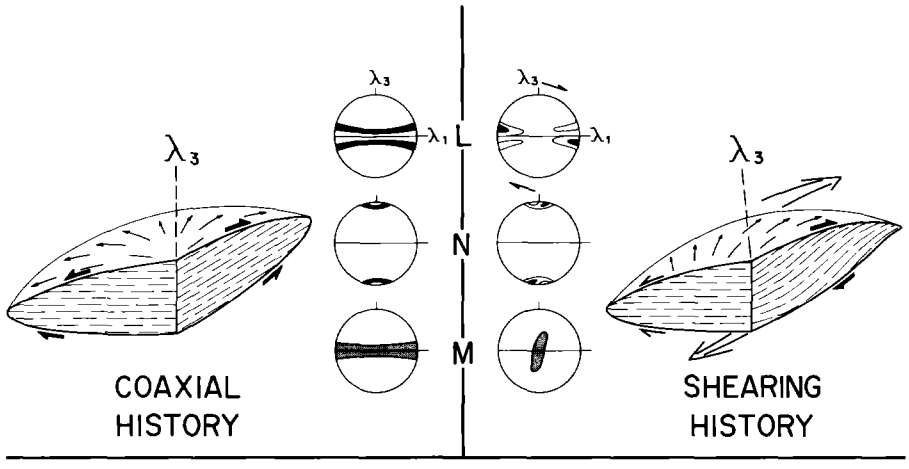

Fig. 10. Sketch summarizing conclusions on relationships between shear zone patterns and bulk deformation history (case of flattening strain); see text for further details.

characterize the $\lambda_1\lambda_3$ plane. The constriction field is expected to yield rod-shaped shear zone patterns.

These variations of shear surface geometry are similar to those of surfaces of no finite stretch and of domains of large shear in the bulk strain ellipsoid. This is consistent with fibre models which predict that a shear surface which provides a significant contribution to the bulk strain should accumulate both maximum parallel shear and minimum parallel stretch.

Our kinematic interpretation of shear zone patterns accounts for a general feature of ductile shear zones: they lie always at high angle (typically around 60–70°) to the direction of principal shortening, in contrast to brittle faults (typically at around 30–40° to λ_3) whose orientation depends largely on mechanical factors. Furthermore, the observed analogy with models of inextensible fibres emphasizes that the rotation of an active shear zone during progressive deformation differs from that of a passive material surface with same initial orientation. However, the condition of inextensibility is indeed an extreme mechanical approximation for shear zones as: (i) it neglects any mechanical control on shear zone initiation and propagation; and (ii) it assumes that, once developed, shear zones are zones of extremely easy slip during the entire subsequent deformation (no strain hardening).

In addition, common features of ductile shear zone patterns are homogeneous straining within domains between shear zones and cross-cutting of one set of shear zones by another. These allow overall stretch and local destruction of individual slip surfaces (see Means 1977).

Bulk deformation history vs shear zone pattern

Our observations emphasize that non-coaxial deformation histories result in asymmetric shear zone patterns, whereas coaxial histories can preserve symmetric patterns during progressive deformation. Basic changes from symmetric to asymmetric patterns are in fact quite similar to those classically used as shear criteria in lattice fabric analysis (Fig. 10). They are marked by: (i) a shift of local shear directions towards the bulk shear direction; and (ii) the predominance of one shear sense over the conjugate sense. It appears that local shear directions and shear senses are modified according to the bulk deformation history, whereas patterns of shear surface orientations continue to bear a relation with the strain ellipsoid shape (Fig. 10). Lens-shaped patterns described in the Gotthard and Kabylie granites support this statement. From the comparison with fibre models, we infer that domains where the deformation is accommodated by slip on a single set of parallel shear surfaces (*C–S* structures) have undergone a bulk progressive simple shearing.

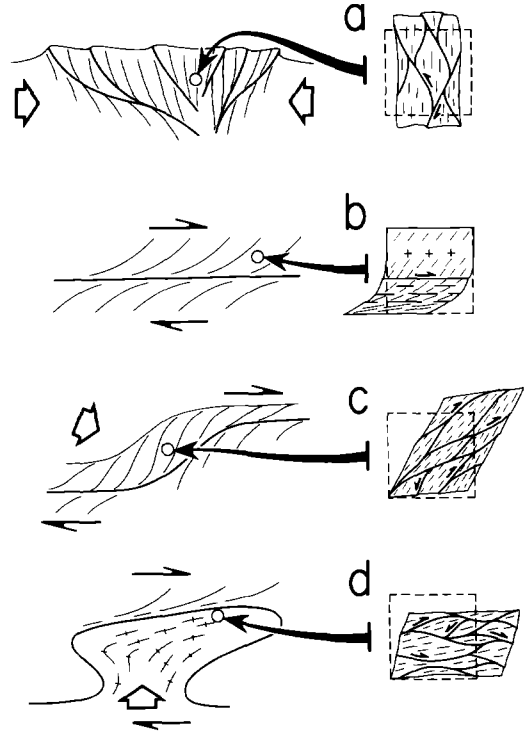

Fig. 11. Sketch illustrating some general aspects of shear-zone patterns ($\lambda_1\lambda_3$ plane) as expected in crustal structures according to the local kinematic history; (a) coaxial shortening; (b) simple shearing; (c) compressive thrusting; and (d) extensional shearing.

Shear zone patterns within crustal structures

The interpretation of shear zone patterns proposed in this paper refers to average kinematics at the scale of the considered pattern. The kinematic history generally varies across a given structure, which introduces some limits in practical applications. Indeed, reliable kinematic inferences require the measurement of a significant number of shear zones within a material that was homogeneously deformed at the bulk scale.

However, shear zone patterns exist at all scales within the crust. They can therefore constitute a unique kinematic indicator from the sample scale to crustal scale. Furthermore, they are generally well developed and readily interpretable in granitic rocks whose initial state was homogeneous and isotropic. They occur commonly in the crust and are often associated with major tectonic events. Shear zone patterns can be used to characterize crustal deformation zones such as coaxially shortened zones (Fig. 11a), large-scale simple shear zones (Fig. 11b), thickened thrust zones (Fig. 11c) or thinned zones (e.g. top of diapir emplaced during regional thrusting (Fig. 11d).

Acknowledgements—W. D. Means's critical comments and reviews by D. G. De Paor and G. Oertel helped to improve the final manuscript.

REFERENCES

Arthaud, F. 1969. Méthode de détermination graphique des directions de raccourcissement, d'allongement et intermédiaire d'une population de failles. *Bull. Soc. géol. Fr.*, 7 *Ser.* **XI**, 729–737.

Bell, T. H. 1981. Foliation development—The contribution, geometry and significance of progressive, bulk, inhomogeneous shortening. *Tectonophysics* **75**, 273–296.

Berthé, D., Choukroune, P. & Jegouzo, P. 1979. Orthogneiss, mylonite and non-coaxial deformation of granites: the example of the South Armorican Shear Zone. *J. Struct. Geol.* **1**, 31–42.

Choukroune, P. & Gapais, D. 1983. Strain pattern in the Aar granite (central Alps): orthogneiss developed by bulk inhomogeneous shortening. *J. Struct. Geol.* **5**, 411–418.

Cobbold, P. R. & Gapais, D. 1987. Slip system domains. I. Plane-strain kinematics of arrays of coherent bands with twinned fibre orientations. *Tectonophysics* **131**, 113–132.

Collins, D. A. & De Paor, D. G. 1986. A determination of the bulk rotational deformation resulting from displacements in discrete shear zones in the Hercynian fold belt of South Ireland. *J. Struct. Geol.* **8**, 101–109.

Dunnet, D. 1969. A technique of finite strain analysis using elliptical particles. *Tectonophysics* **7**, 117–136.

Flinn, D. 1962. On folding during three dimensional progressive deformation. *Q. Jl. geol. Soc. Lond.* **118**, 385–433.

Freund, R. 1974. Kinematics of transform and transcurrent faults. *Tectonophysics* **21**, 93–134.

Frey, M., Bucher, K., Frank, E. & Mullis, J. 1980. Alpine metamorphism along the geotraverse Basel-Chiasso: a review. *Eclog. geol. Helv.* **73**, 527–546.

Gapais, D. & Jegouzo, P. 1985. Domainal orientations of *C–S* structures in sheared granites (South Armorican Shear Zone). *Int. Conf. on Tectonic and Structural Processes*. Utrecht, 11–13 April 1985, 76–77 (abstract).

Gapais, D. & Cobbold, P. R. 1987. Slip-system domains. II. Kinematic aspects of fabric developments in polycrystalline aggregates. *Tectonophysics*. In press.

Hoeppener, R., Kalthoff, E. & Schrader, P. 1969. Zur physikalischen tektonik. Bruchbildung bei verschiedenen affinen deformationen im experiment. *Geol. Rdsch.* **59**, 179–193.

Jeannette, D. 1972. Analyse tectonique de formations précambriennes. Etude du Nord-Est de la Bretagne. *Sci. Géol Strasb.* **36**, 1–175.

Lagarde, J. L. & Choukroune, P. 1982. Cisaillement ductile et granites syntectoniques: l'exemple du massif hercynien des Jebilet (Maroc). *Bull. Soc. géol. Fr.* 7 *Ser.* **XXIV**, 299–307.

Lister, G. S., Paterson, M. S. & Hobbs, B. E. 1978. The simulation of fabric development in plastic deformation and its application to quartzites: the model. *Tectonophysics* **45**, 107–158.

Logan, J. M., Higgs, N. G. & Friedman, M. 1981. Laboratory studies on natural gouge from the U.S. Geological Survey Dry Lake Valley No. 1 Well, San Andreas Fault Zone. In: *Mechanical Behavior of Crustal Rocks* (edited by Carter, N. L., Friedman, M., Logan, J. M. & Stearns, D. W.). *Geophys. Monogr.* **24**, 121–134.

Mahjoub, Y. & Gapais, D. 1985. Orthogneiss development within thrust zones: an example from eastern Kabylia (Algeria). *Terra Cognita* **5**, 257 (abstract).

Mandl, G., De Jong, L. N. J. & Malltha, A. 1977. Shear zones in granular material. *Rock Mech.* **9**, 95–144.

Marquer, D. 1987. Transferts de matière et dèformation progressive des granitoides. Exemples des massifs de l'Aar et du Gotthard (Alpes centrales suisses). *Mém. docums CAESS*, Rennes, France **10**, 1–250.

Marquer, D. & Gapais, d. 1985. Les massif cristallins externes sur une transversale Guttanen—Val Bedretto (Alpes Centrales): structures et histoire cinématique. *Cr. hebd. Séanc. Acad. Sci., Paris* **301**, 543–546.

Means, W. D. 1977. A deformation experiment in transmitted light. *Earth Planet. Sci. Lett.* **35**, 169–179.

Mitra, G. 1979. Ductile deformation zones in Blue Ridge Basement rocks and estimation of finite strains. *Bull. geol. Soc. Am.* **90**, 935–951.

Oertel, G. 1965. The mechanism of faulting in clay experiments. *Tectonophysics* **2**, 343–393.

Platt, J. P. & Vissers, R. L. M. 1980. Extensional structures in anisotropic rocks. *J. Struct. Geol.* **2**, 397–410.

Priour, D. 1985. Genèse des zones de cisaillement. Application de la méthode des éléments finis à la simulation numérique de la déformation des roches. *Mém. Docums CAESS*, Rennes, France **4**, 1–157.

Ramsay, J. G. 1967. *Folding and Fracturing of Rocks*. McGraw-Hill, New York.

Ramsay, J. G. 1980. Shear zone geometry: a review. *J. Struct. Geol.* **2**, 83–99.

Reches, Z. 1983. Faulting of rocks in three-dimensional strain fields. II. Theoretical analysis. *Tectonophysics* **95**, 133–156.

Simpson, C. 1983. Strain and shape-fabric variations associated with ductile shear zones. *J. Struct. Geol.* **5**, 61–72.

Simpson, C. & Schmid, S. 1983. An evaluation of criteria to deduce the sense of movement in sheared rocks. *Bull. geol. Soc. Am.* **94**, 1281–1288.

Steck, A. 1968. Die alpidischen Strukturen in den zentralen Aaregraniten des westlichen Aarmassivs. *Eclog. geol. Helv.* **61**, 19–48.

Steck, A. 1984. Structures de déformations tertiaires dans les Alpes Centrales (transversale Aar-Simplon-Ossola). *Ecolg. geol. Helv.* **77**, 5–100.

Taylor, G. I. 1938. Plastic strain in metals. *J. Inst. Metal.* **62**, 307–324.

Tchalenko, J. S. 1970. Similarities between shear zones of different magnitudes. *Bull. geol. Soc. Am.* **81**, 1625–1640.

Truesdell, C. & Toupin, R. 1960. The classical field theory. In: *Handbuch der Physic. Encyclopedia of Physics* (edited by Flugge S.) **3**, 226–793.

Watterson, J. 1968. Homogeneous deformation of the gneisses of Vesterland, South-West Greenland. *Bull. Grønl. geol. Unders.* **175**, 1–78.